



A method of autonomous locomotion for mobile robots

Kiyoshi Komoriya , Susumu Tachi & Kazuo Tanie

To cite this article: Kiyoshi Komoriya , Susumu Tachi & Kazuo Tanie (1986) A method of autonomous locomotion for mobile robots, Advanced Robotics, 1:1, 3-19, DOI: [10.1163/156855386X00283](https://doi.org/10.1163/156855386X00283)

To link to this article: <https://doi.org/10.1163/156855386X00283>



Published online: 02 Apr 2012.



Submit your article to this journal 



Article views: 59



View related articles 



Citing articles: 13 View citing articles 

A method of autonomous locomotion for mobile robots

KIYOSHI KOMORIYA, SUSUMU TACHI and KAZUO TANIE

*Mechanical Engineering Laboratory, Ministry of International Trade and Industry, Tsukuba
Science City, Ibaraki 305, Japan*

Received for *JRSJ* 3 April 1984; English version received 26 March 1985

Abstract—A navigation method is presented which enables a mobile robot to perform autonomous locomotion. The feasibility of this method was demonstrated using experimental hardware—a prototype robot with ultrasonic sensors.

This method uses objects of simple shape, such as poles and flat surfaces of walls selected from the environment, as landmarks and a map which indicates the relations of these landmarks. The robot moves from a given point to another along a designated path using its sensors. At each point it measures the positions of the objects selected as landmarks and corrects its path.

The following basic problems encountered in realizing this method are discussed: (a) path design connecting two points in the environment; (b) the control of the robot's path; (c) measurement of the objects' positions using an ultrasonic sensor; and (d) correction of error from the designated path.

To navigate a mobile robot it is necessary to be able to control it so that a specified path is followed accurately. Since absolute positional information is not available, the mobile robot must obtain accurate positional data from its surroundings. The method uses natural objects to gain such information. Its advantages include: (a) reduction in the investment of equipment for the supply of positional data; and (b) simplification of the object detection problem by giving information on the objects.

1. INTRODUCTION

Navigation technology to guide a mobile robot is essential for the realization of independent locomotion of mobile robots as well as for construction of the locomotion mechanism and robot control. The basic technology is designed in such a way as to enable correct tracing of a designated path. Owing to its mobility, the control of mobile robots is different from finger-tip trajectory control of a manipulator which has a base point in the working space. To inhibit deviation from the given path the base point must be set in the environment. For example, induction cables [1] and metal tapes [2] are used as base points for unmanned carrier carts used in factories and warehouses.

Methods that provide stationary base points have the disadvantage that equipment built into the floor has less navigational flexibility and a large initial investment is required to construct the path route. In addition, the guidance method, which uses interior sensors such as encoders installed in the wheels, cannot be used independently except for short-range applications in which deviation is allowed because this method cannot prevent deviation. A mobile system with higher independence [3-6], in which the robot navigates determining base points by recognition of its own environment, is ideal, but present pattern recognition technology does not enable the realization of such a system.

On the basis of the present technological situation mentioned above, we have proposed a navigation system [7] that uses rectangular, monocolored tape called

“landmark” installed on the floor. The layout is given to the robot as environmental information (map). Optical sensor detection enables navigational errors to be corrected and the position to be recognized. This method intends to solve the problems of the two systems by combining locomotion control between landmarks using interior sensors, and correcting navigational errors from the target path route at landmark base points. Although the shape of the landmarks is simple, the use of artificial objects requires equipment investment for the environment.

Therefore, we propose in this paper a navigation system, developed from the distributed landmark system, which senses and uses cylindrical objects and flat faces of buildings in the environment instead of artificial objects. We attempt to verify the procedure experimentally using a test robot with encoders as interior sensors, which determine the steering angles and turning angles of the wheels, and ultrasonic sensors as exterior sensors. Herein, we focus on the essential points of the system: (a) the use of interior sensors to enable navigation between two points; (b) exterior sensors to detect cylindrical and flat face objects; and (c) information to correct navigational deviations.

2. NAVIGATION METHOD USING DISCRETE LANDMARKS

The navigation method using discrete landmarks assumes base point marks at each marked point. Specifically, passing points are assumed at key points in the navigation environment, such as intersections of passages, and landmarks are determined in the vicinity of each passing point. The passing point and landmark information is given to the mobile robot in the form of a ‘map’.

The passing point information in the map includes the code of each passing point, the positional coordinates expressed by the fixed coordinates established in the environment, and the vector describing the path direction at the passing points. The adjacent passing point codes which constitute the path are also given. Information on the direction of the path is given to predetermine the direction of the robot so that the robot can detect the landmarks easily and pass along narrow paths. The landmark information includes the cylindrical poles and flat building surfaces, and their positional coordinates compared with fixed coordinates.

The first navigation step is to determine the array of passing points that constitute the path to the given destination point by carrying out a search in the map. Selection of one array of passing points from the number of arrays obtained from so-called tree-structure searching is conducted on the basis of a given appropriate evaluation function. Then the path between neighbouring passing points is determined before the operation is started, and navigation is controlled by the interior sensors. At each passing point, a sensor located on the robot scans the direction in which the next landmark is expected, and identifies the landmark according to the information obtained. Then the navigational error is determined using the relative positional information and, in order to cancel the error, the path to the next passing point is redesigned.

This method allows the path to be partially changed by establishing an appropriate additional passing point between the two predetermined neighbouring passing points. A navigation system that has great freedom and avoids obstacles is thus possibly realized.

3. PATH NAVIGATION BETWEEN PASSING POINTS

3.1. Design of the path between two passing points

The path between two passing points is designed to guide a mobile robot from a starting point S in the direction indicated by the vector s to a target point D in the direction of vector d (Fig. 1).

The paths of wheeled robots may be restricted because of the wheel arrangement. For example, two-wheel drive, commonly used for mobile robots, permits freedom in the selection of paths by controlling the direction of rotation and the speed ratio of the two wheels. However, both tricycle configuration and four-wheel arrangement, such as that used for automobiles, have a basic movement with its centre at the intersection of the front and rear wheel shafts which inhibits a change of position and attitude independently. The latter wheel arrangements allow more accurate trajectory control than the former power-wheeled steering-type because of the distance between the front and rear wheel shafts, that is, the wheel base.

Now let us discuss the motion from s to d shown in Fig. 1. In the former case, the robot orients itself in the direction SD without changing its position, and moves to D. Changing its attitude in the direction of d at point D allows easy navigational control for the shortest distance travelled. However, the travelling time becomes

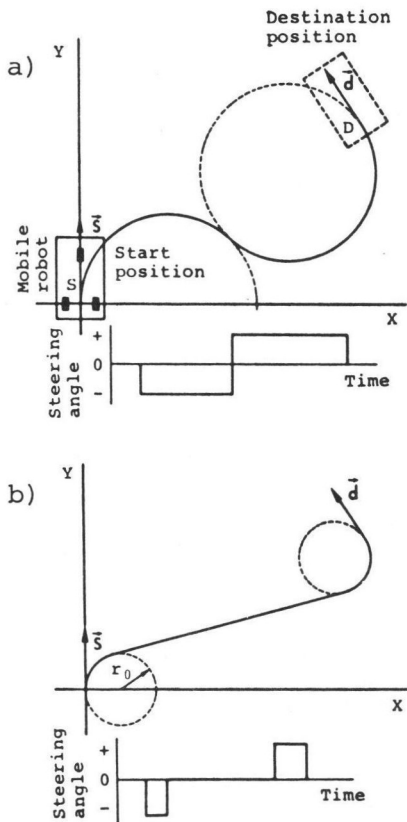


Figure 1. Basic path design.

longer if the time required to change its attitude is included. The three- and four-wheel types, which cannot manoeuvre such paths, are not assumed to be inferior to the former type, depending on the evaluation criteria. With this in mind, we discuss a path design for the latter type of mobile robot which enables potentially accurate trajectory control.

The basic trajectory of the latter type is an arc, made possible by maintaining a stable front-wheel steering angle. As shown in Fig. 1(a), the path may be constructed by two circles contacting **s** and **d** at their starting points, respectively, and at the same time contacting each other. When the radii of the two circles are equal, steering control is accomplished by switching, at the contact point, the steering angle to the opposite direction, and simplified control results. However, the drawback of this method is that the change of the steering angle is dependent on the location of **d**, the accuracy of switching the steering position decreases as **d** becomes further away, and deviation from SD increases. This produces difficulties when path selection is limited. Therefore, as shown in Fig. 1(b), the path route is modified so that it consists of an arc and a straight line. The path is determined by circles of radius r_0 , each of which contacts the starting points of **s** and **d**, and the common tangential line. At this time, upon assuming that the steering angle corresponding to r_0 is θ_0 , steering control is attained by switching at certain times the three values $+\theta$, $-\theta$ and 0, while monitoring the distance moved. The value θ can be defined as the value at which slippage between the wheels and the path surface becomes minimal under the influence of the centrifugal force determined by the travelling speed, not by the position of **d**. If r_0 is decreased, the deviation from the shortest path SD is also reduced.

Next, we will discuss how to determine the position at which the steering should be changed. Two circles of a certain radius contact the vectors **s** and **d** at their starting points, and there are four common tangential lines for each combination as shown in Fig. 2. Depending on the directions of **s** and **d**, only one tangential line is available for each combination. Then by checking the four tangential lines for each combination, one line is selected. Although the line that does not collide with the environment can be selected, the line that provides the shortest path is selected for a reasonable solution in this paper. The point at which the steering angle should be changed is obtained from the lengths of the arc and the tangential line. These algorithms enable the path to any given **d** to be determined.

The above path design method is based on an ideal navigation system. In practice, it is difficult to trace the path shown in Fig. 1(b) because of errors caused by many factors including the response delay of the steering system, steering control error, deviation of the point at which steering must be changed due to an error in the drive distance meter, slippage due to inertial force, and dimensional errors of mechanical structures. In this paper we attempt to correct the steering system delay, which constitutes a large proportion of the errors. The errors caused by the other factors are corrected by the landmark reference at the passing points.

Figure 3(a) shows the ideal response of the steering control system together with the actual response. As can be seen, there is a small time lag before the steering angle reaches the determined angle. The trajectory from the starting point of the steering operation does not form an arc. The actual trajectory is obtained from equations (1)–(3), which represent the motion compared with the steering angle $a(t)$ of the mobile robot.

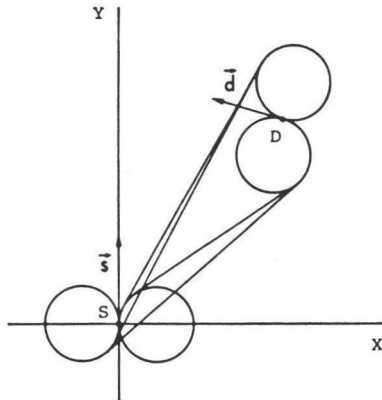


Figure 2. Possible paths from S to D.

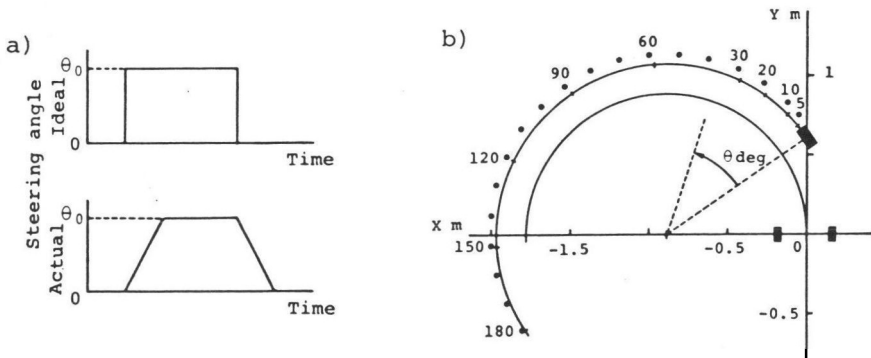


Figure 3. Steering response and the position error from the basic path.

$$\beta(t) = \beta_0 + v/l \int_0^t \sin(a) dt \quad (1)$$

$$x(t) = x_0 + v \int_0^t \cos \{a(t) + \beta(t)\} dt \quad (2)$$

$$y(t) = y_0 + v \int_0^t \sin \{a(t) + \beta(t)\} dt \quad (3)$$

v is the driving speed, l is the wheel base, $\beta(t)$ is the angle of attitude, and $(x(t), y(t))$ are the coordinates of point C at which the front wheel contacts the ground. The subscript 0 indicates the initial value.

Figure 3(b) shows the trajectory points of C compared with the steering angle θ , which is the final point when the attitude is turned by θ by steering from 0 to θ and returning to 0. The response of the steering control system is assumed to be that shown in the lower graph of Fig. 3(a). If the time required for the robot to change its attitude by θ is assumed to be t_θ , the error $e(\theta)$ between the actual trajectory and an ideal circular one when the attitude is required to be changed by θ is represented by the equations

$$\beta(t_\theta) = \theta \quad (4)$$

$$\mathbf{e}(\theta) = \begin{bmatrix} e(\theta)_x \\ e(\theta)_y \end{bmatrix} = \begin{bmatrix} x(t_\theta) - r_0(\cos \theta - 1) + l \sin \theta \\ y(t_\theta) - l(\cos \theta - 1) - r_0 \sin \theta \end{bmatrix}. \quad (5)$$

If the error is taken into consideration, the aforementioned path is corrected as shown in Fig. 4. First, the attitude angle is altered by θ_1 at the first curve, then the straight line is followed and the attitude is again changed by θ_2 at the second curved portion. Assuming the errors at the two curved portions to be $e(\theta_1)$ and $e(\theta_2)$, the final error is obtained from the equation

$$\mathbf{e}_f = \begin{bmatrix} e_{fx} \\ e_{fy} \end{bmatrix} = \begin{bmatrix} e(\theta_1)_x + e(\theta_2)_x \cos \theta_1 - e(\theta_2)_y \sin \theta_1 \\ e(\theta_1)_y + e(\theta_2)_x \sin \theta_1 + e(\theta_2)_y \cos \theta_1 \end{bmatrix}. \quad (6)$$

As the error e_f can be calculated in advance, the path that will lead the robot correctly to the next passing point can be determined by iteration of the path design, correcting the passing point by e_f . The paths mentioned above are designed for the experimental mobile robot given below, but can be used for other wheel-type mobile robots, e.g. two-wheel-drive robots.

3.2. Travelling experiments

Table 1 gives the specifications of the mobile robot used in the travelling experiments, and Fig. 5 shows its appearance. The robot is a front-wheel driven and steered tricycle vehicle which uses battery power. Motion is controlled by a DC-motor speed control connected to the front wheel, and a digital position control steering which rotates the front wheel about its vertical axis. Two rear wheels rotate

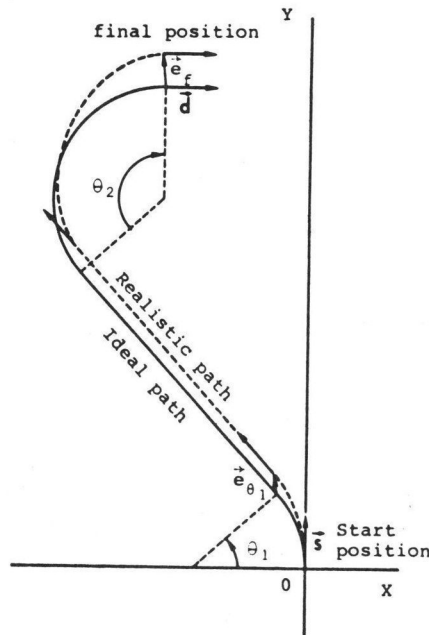


Figure 4. Correction of the basic path.

independently, and the encoders installed in them detect how much the wheel is turned so that the distance travelled can be calculated. An LSI-11 microcomputer on the robot controls the travelling system and the ultrasonic sensors.

Table 1.
Specifications of the prototype mobile robot

Size:	length	0.94 m
	width	0.555 m
	height	0.625 m
	wheel base	0.60 m
	distance between rear wheels	0.337 m
Weight:		69.2 kg
Drive:	front wheel drive and steer computer control	
	drive motor	100 W
	steering motor	30 W
Power:	nickel-cadmium battery	12 V×35 A h
Computer:	LSI-11 32 kW memory 4ch-digital I/O 16ch-ADC, 4ch-DAC cassette tape (TU58) terminal (Profort 801)	

In the experiment the robot travels along the path to the target position under the control of the microcomputer, which checks the distance travelled and alters the steering according to the off-line calculated course data. Then the final position of the robot is measured. Figure 6 gives an example of the path design and the final position of the robot when a target vector was set 3 m ahead and in the right direction. Figure 6(a) shows the ideal path and the results of the course data without correction. As shown in the figure, the deviation from the target point becomes larger as the speed

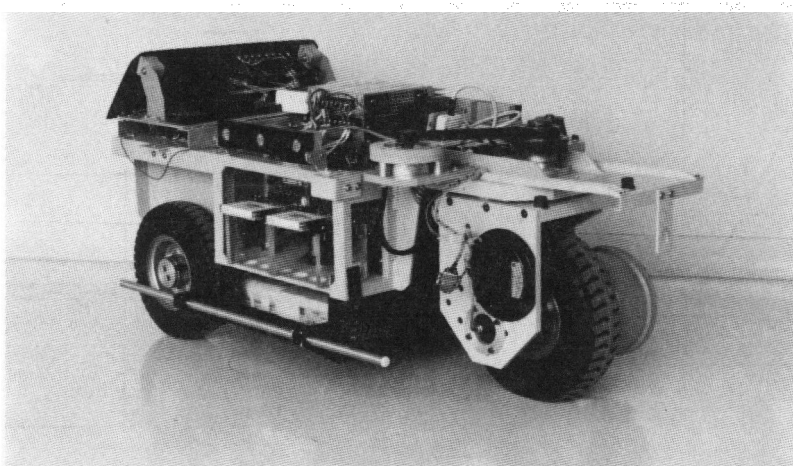


Figure 5. A prototype mobile robot.

increases, but it was apparent that the reproducibility was high. Figure 6(b) shows the navigation results when the robot was controlled to follow the dotted line of Fig. 4 which was adjusted for the delay in steering response. The figure shows that the final positions of the robot vary depending on the speed. In all the cases, however, the final attitude error was within 2° . Figure 6(c) shows the results in the case of the path design by convergence calculation which enables travelling to the target point with a small deviation. Less than five convergence calculations were necessary to design the path. The results show that accurate navigation to the target point is possible regardless of the speed.

4. ULTRASONIC MARK POSITION MEASURING METHOD

4.1. Sensor construction and the measurement principle

Vertically uniform, pillar-shaped bodies such as rectangular furniture and cylindrical poles, are assumed as the objects of the sensors, or marks, and their sections are assumed to be circles or concave polygons. On the basis of this assumption, the sensors must be capable of detecting the objects in two-dimensional space. Then the transmitter and receiver elements are arranged as shown in Fig. 7. 'T' in the centre is the transmitter element with receiver elements R_i arranged in a straight line, evenly

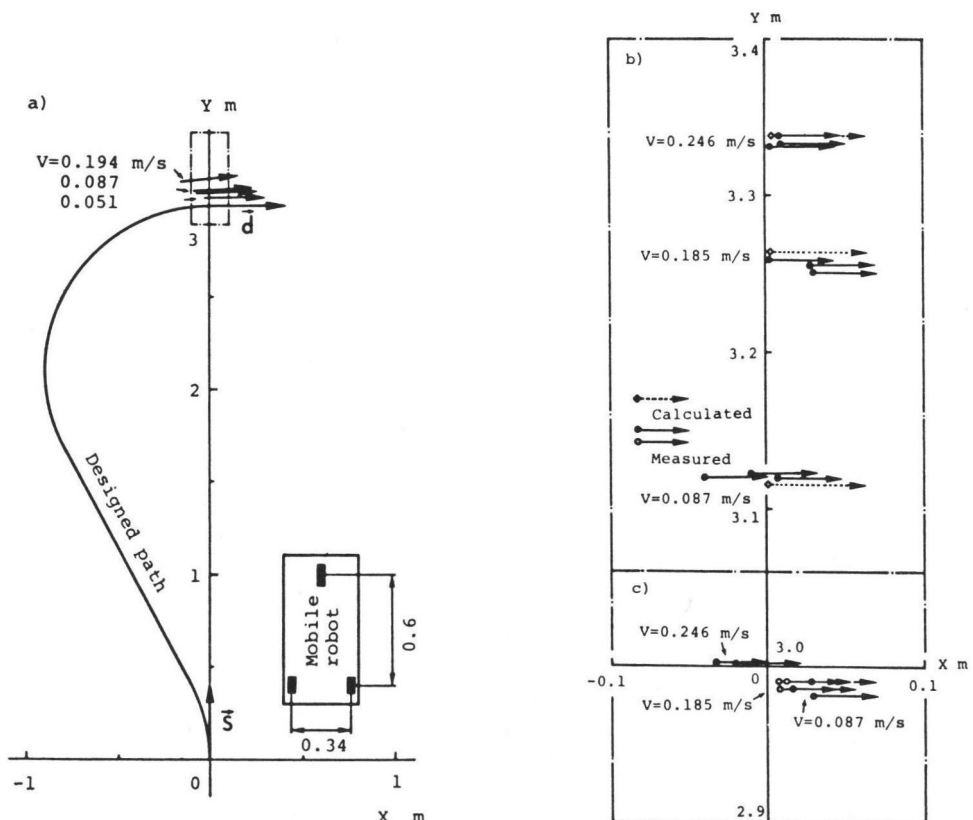


Figure 6. Experimental results of the path: (a) using the basic path design; (b) using the corrected path design; and (c) using the final path design.

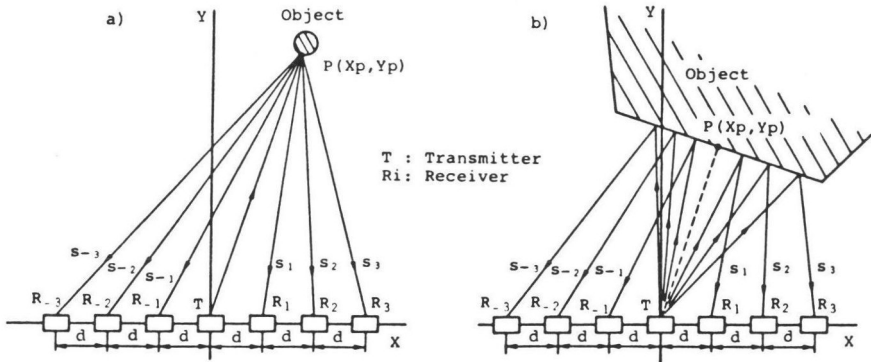


Figure 7. Construction of an ultrasonic sensor and two-type objects.

spaced to the left and right of T . The transmitter and receiver elements are positioned so that their axes are perpendicular to the axis of the sensor array and parallel to each other. Each R_i receives the ultrasonic wave transmitted from T and reflected by an object, and indicates the distance s_i obtained from the elapsed time from transmission to reception. To obtain the position of the object (x_0, y_0) from s_i , the shape of the object must be known. Even if the shape of the object is assumed to be a circle of radius r , complicated computations are required to determine r and its centre (x_0, y_0) accurately. It is very difficult to obtain an accurate value of r because of the error involved in s_i . Therefore, we will try to determine a point $P(x_p, y_p)$ on the surface of the object nearest to T , and the distance S between T and P .

(a) Assuming the object to be a circle of radius 0, or a point, we obtain S and (x_p, y_p) from the following formulae:

$$S = \frac{ij(i-j)d^2 - (js_i^2 - is_j^2)}{2(is_j - js_i)} \quad (7)$$

$$x_p = \frac{(i^2s_j - j^2s_i)d^2 - s_r s_j(s_i - s_j)}{2d(is_j - js_i)} \quad (8)$$

$$y_p = \sqrt{S^2 - x_p^2} \quad (9)$$

where i and j represent the number of sensors, d is the distance between the elements and s_i is the distance from T to R_i via the surface. When the number of pieces of receiver elements used is k , a maximum number ${}_k C_2$ of (x_p, y_p) values are available. Then averaging is done to improve the reliability and accuracy of the data. There are two averaging methods: (1) the receiving intensity is used as the weight; and (2) the distance between the receiver elements is used as the weight since higher accuracy can be obtained from a long triangulation base-line. For example, assuming the receiving levels of receiver elements R_i and R_j to be I_i and I_j , the weight for the pair of i and j becomes

$$W_{ij} = I_{ij} / \sum_{k, l=1, \pm 2, \dots, \pm n} I_{kl};$$

assuming $I_{ij} = I_i * I_j$, the weight of the latter becomes

$$W_{ij} = \frac{|i-j|}{\sum_{k,l=\pm 1, \pm 2, \dots \pm n} |k-l|}.$$

By averaging these two values further, the position of the object is obtained from the following formulae:

$$x_{pm} = a(\sum W_{ij} x_{pij}) + \beta(\sum W_{ij} x_{pj}) \quad (10)$$

$$y_{pm} = a(\sum W_{ij} y_{pij}) + \beta(\sum W_{ij} y_{pj}) \quad (11)$$

where $a+\beta=1$ and averaging should be done for every pair of i and j .

(b) If the object is assumed to be a circle of infinite radius, i.e. a straight line, each R_i receives the reflected signal from the mirror position of T against that straight line. In this case, S and (x_p, y_p) are calculated from equations (12)–(15):

$$(2x_p - id)^2 + (2y_p)^2 = S_i^2 \quad (12)$$

$$S = \sqrt{\left[\frac{1}{2n} \left(\sum_{i=-n}^n S_i^2 - \sum_{i=-n}^n i^2 d^2 \right) \right]} \quad (13)$$

$$x_p = \frac{1}{2n(n+1)} \left(\sum_{i=-1}^{-n} S_i^2 - \sum_{i=1}^n S_i^2 \right) \quad (14)$$

$$y_p = \sqrt{(S^2 - x_p^2)}. \quad (15)$$

The direction of the straight line is obtained from $-x_0/y_0$.

4.2. Numerical simulation

The effects of the number of receiver elements, the curvature of the object, and the error in the distance measured by the elements on the detection of the position of the object are discussed using numerical computation by the two algorithms mentioned above.

The position of the object was determined on a straight line at an angle of 20° to the Y -axis as shown in Fig. 8, as a severe condition to consider the directivity of the ultrasonic sensing elements. The length was taken up to $y=20$ in the forward direction, assuming the normalized width of the sensor to be 2. The curvature of the object, in contrast to the computation assumption, was used. That is to say, a straight line was used for the object in case (a) and a circle of radius 0.1 in case (b).

With the conditions specified above, the influence of the number of elements was investigated based on the assumption that there is no error in the distance measured for each element. The results of both methods showed that the error in detecting the position of the object decreases as the number of elements increases. But no noticeable difference was observed in terms of numerical values, where the error in the x -direction was less than 0.8% of the measured distance, and less than 0.6% in the y -direction, even when only one element was used on a side. To investigate cases where there are errors in the measured distances of elements, the mean value and the standard deviation of the detected position were checked by giving errors obtained from random numbers with a uniform density distribution. Multiples of 0.0241 by integer numbers (n) were used for the maximum error amplitude, which corresponds to half the wavelength of the ultrasonic wave used by the hardware mentioned below. Figure 8 shows the results with the standard deviation enlarged ten times in the case

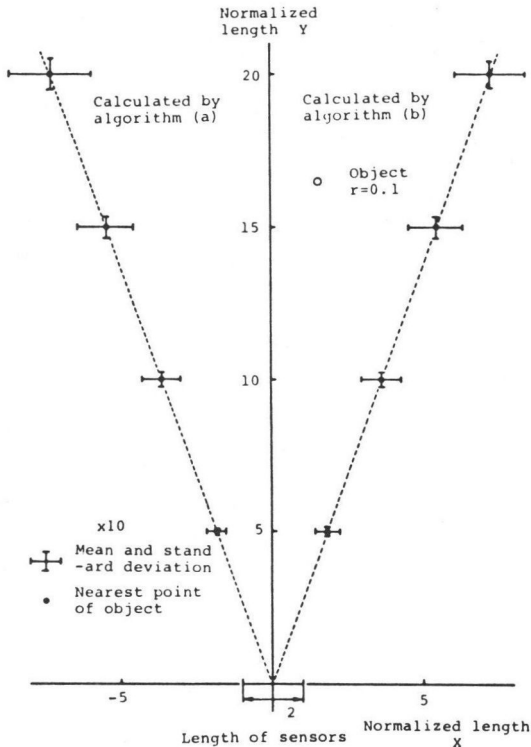


Figure 8. Simulation of position measurement using the ultrasonic sensor.

where four receiver elements were used on one side with $n = 1$. Figure 8(a) represents the results of method (a) and Fig. 8(b), those of method (b). It can be seen that the standard deviation of method (a) is smaller for a short distance than that of method (b), and is greater for long distances. There is no noticeable difference between the two methods. The values are less than 1.9% of the measured distance in the x -direction for method (a) at $y=20$, and less than 0.25% in the y -direction.

4.3. Experimental apparatus

The hardware shown in Fig. 9 was developed for performance evaluation of the ultrasonic mark position measuring method based on the above-mentioned principle. Fig. 10(a) is a block diagram of the apparatus, and Fig. 10(b) is the timing chart. One transmitter element (EFR-OBS40K2) having a resonance frequency of 40 kHz and eight receiver elements (EFR-RSB40K2; Matsushita Tsushinki Kōgyo Ltd.) were placed 5 cm apart to form a sensor. A PDP-11/44 minicomputer was used to control the signal through a parallel interface. With the interface section replaced by that of a microcomputer, the experimental apparatus was easily installed on the mobile robot, and the same software as that used by the minicomputer was used. The apparatus was operated in the following way. Start pulses were sent from the output buffer of the parallel interface, then a trigger burst wave of the 40 kHz carrier was sent to the receiver elements. At the same time, the same signal reset the time measuring counters. The reflected wave detected by the receiver elements underwent amplification and band path filtering twice, then it was rectified to produce a stop

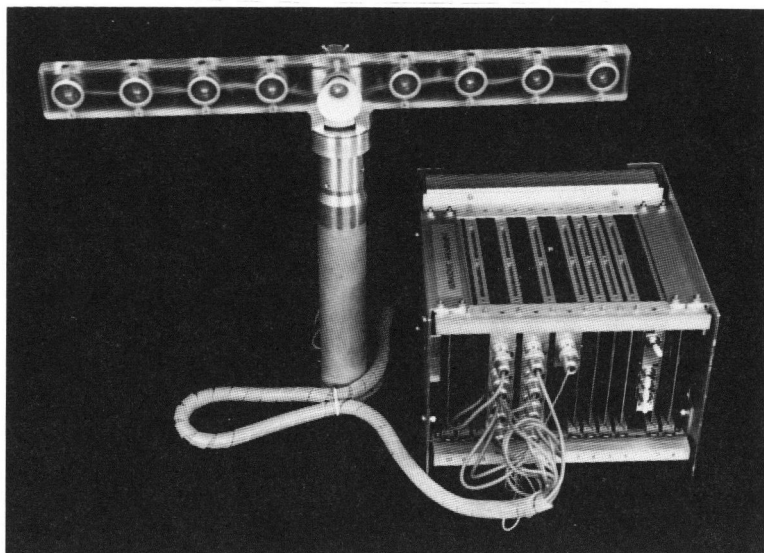


Figure 9. A prototype ultrasonic sensor.

signal for the time measuring counters by the comparator. A pulse wave of 226.7 kHz was used for the time measuring clock, and 12-bit counters allowed distances of up to approximately 3 m to be measured. To preclude possible erroneous operation as a result of the direct transmission wave, after transmission a non-response period was given to the stop-signal generating section. Theoretically, the wave reflected from the nearest object was detected, and when no reflected wave was received, the overflow of the counter stopped the clock input. Twenty milliseconds after transmission, the 'ready' signal was sent to the computer, which read the data in the counter, scanning the multiplexer progressively to obtain the position of the object; the software executed the processing thereafter.

4.4. Position measurement experiments

Prior to the distance measurement experiments, preliminary tests were conducted to calibrate the measured distances and to check the real-time characteristics of the sensor system. For the calibrations a flat metal plate (21 cm square) was placed at several points on the axis of the transmitter elements, and the data obtained by each channel and actual distances were approximated by the linear function for calibration. The same metal plate was used to check the real-time characteristics. The metal plate, or an object, was moved linearly in front of the transmitter elements and the distance was measured on-line. At the same time, the position of the LED installed on the object was measured from the lateral direction using SELSPOT system, position measuring equipment incorporating a PSD (Position Sensitive Detector). Then the results of the two measurements were compared. The speed of the object was 0.3 m s^{-1} . A satisfactory response and accuracy were obtained.

A plastic foam cylinder (dia. $16 \times 23 \text{ cm}$) was used as the object for the distance measurement experiments. The cylinder was supported with its axis vertical and it moved in two dimensions for measurement of the position. In the averaging of

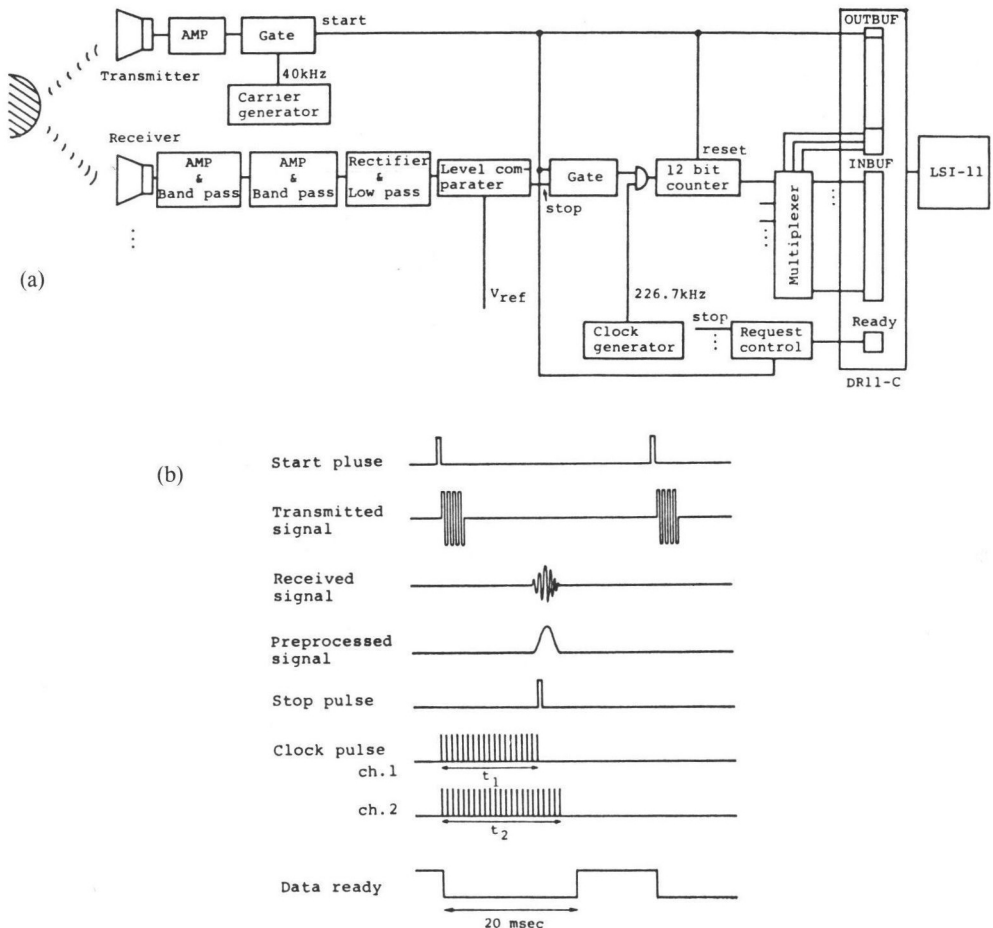


Figure 10. (a) Block diagram of the ultrasonic sensor. (b) Timing chart of the ultrasonic sensor.

method (a), average of the intensity signal needs an extra hardware, such as AD convertor, to get the intensity data. That may make the system very complicated. Therefore, time-sequenced data were gathered and channels with a small variance were selected to be employed with only those averages which used the distance between the receiver elements as the weight. Figure 11(a) shows the effects of the averaging. The dots in the figure are the measurement results of each sensor pair; the symbol X indicates the position of the object after averaging. Two points in the figure are very close to the actual position (+). Figure 11(b) shows the results of the accuracy investigation within the detection area determined by the directivity of the sensors. The symbol + represents the real position and the dots represent the measured positions. As observed from the figure, although the error increases as the distance becomes larger, the error falls within 10 cm over an area 1 m wide and 2.5 m long.

The measurement results of method (b) are shown in Fig. 11(c). Results similar to those of method (a) are observed. The deviations fall within 10 cm over the area shown in the figure. The position of the cylinder shown in the figure is the nearest point on the cylinder surface to the sensors.

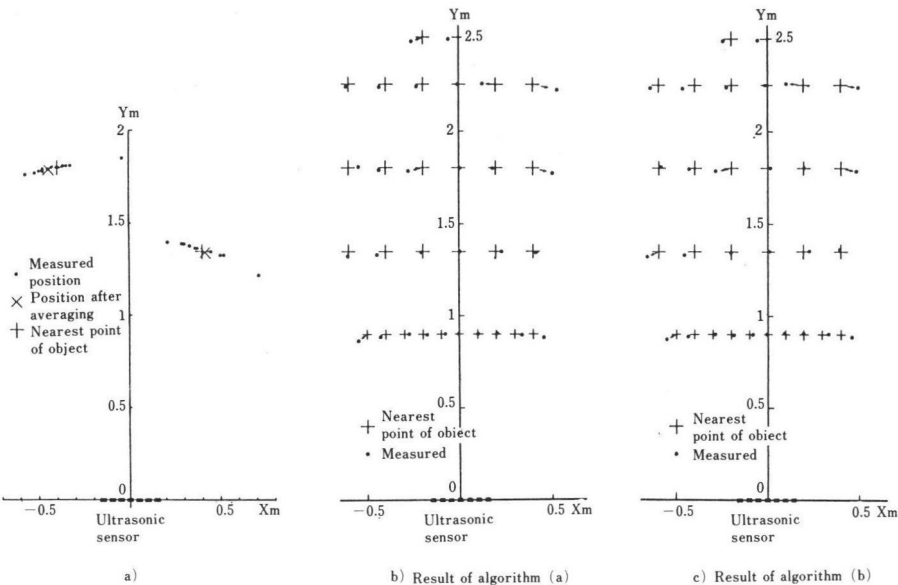


Figure 11. Experimental results of position measurement using the ultrasonic sensor.

5. CORRECTION OF THE TRAVELLING ERROR USING ULTRASONIC MARK POSITION MEASURING EQUIPMENT

In this section a method is discussed which measures the position of a cylinder using the sensor mentioned in Section 4.1, and uses the data measured to detect positional errors produced by the motion. It is a travel error correction method that employs objects in the operation environment.

Figure 12 shows the measuring method. To calculate the relative position easily, a straight travel path is used for the measurement. For higher measuring accuracy, a number of measuring points were selected at locations symmetrical about the origin of the $O-XY$ system of coordinates determined on the path at even-spacing. The shortest distance s_i from each measuring point to the object is measured. The location of the object (X_0, Y_0) about $O-XY$ coordinates and the radius r are given in advance

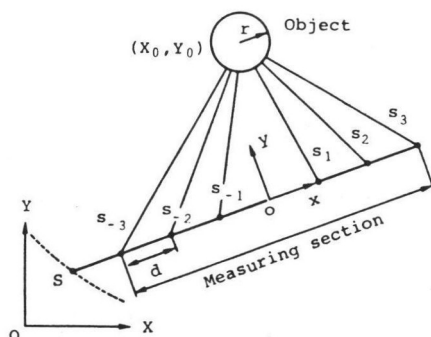


Figure 12. One method to measure an object as a mark.

as part of the environmental information. Using r , the position of the given object (x_m, y_m) about the $o-xy$ coordinates is obtained from the following equations:

$$x_m = \frac{1}{2n(n+1)d} \left\{ \sum_{i=1}^n s_{-i}^2 - \sum_{i=1}^n s_i^2 - 2r \sum_{i=1}^n (s_i - s_{-i}) \right\} \quad (16)$$

$$y_m = \sqrt{\left[\frac{1}{2n} \left\{ \sum_{i=1}^n (s_i + r)^2 + \sum_{i=1}^n (s_{-i} + r)^2 \right\} - \frac{1}{6}(n+1)(2n+1)d^2 - x_m^2 \right]} \quad (17)$$

where n is the number of measuring points on one side.

An experiment was conducted to investigate the performance of the ultrasonic mark position measuring equipment mentioned above. A cylinder made of paper of radius 0.175 m and height 0.43 m was used as the object, and the distance was measured using the ultrasonic sensor on the mobile robot mentioned in Section 3.2. As shown in Fig. 13, the object was positioned 1 m to the left of the path, and the position was measured by the ultrasonic sensor on the mobile robot, which travels in the positive direction of the Y -axis, at 40 points ($n=20$) over a distance 0.5 m. Three starting points, estimated from measurements with the real starting point, are indicated in the figure. It was recognized that even a simple sensor like the one used for this test enables distances to be measured with errors of less than 2 cm.

Although this test uses information that the path is parallel to the Y -axis, the direction of the path is generally unknown and the position of a moving object about $O-XY$ coordinates cannot be determined solely from (X_0, Y_0) and (x_m, y_m) information. Therefore, the starting point of a linear path S , for example, is estimated to be on an arc having its centre at the centre of the object, as shown in Fig. 12.

Next, we will discuss the method for determining the position S on the dotted line.

(i) To select more than one object, to obtain arcs on which there is a point S corresponding to each object, and to determine the position of S at the intersection of the arcs. However, it is not practical to select a number of objects that can be measured simultaneously.

(ii) To estimate the direction on arrival at point S using information from the

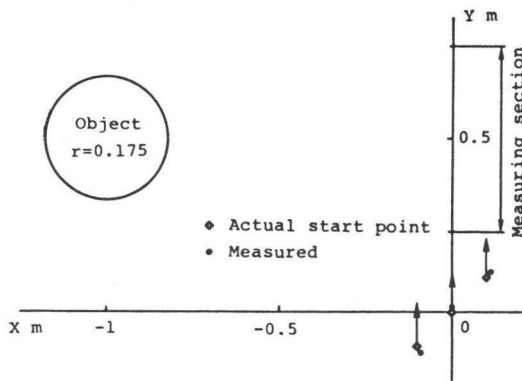


Figure 13. Experimental results of the error detection from the designated path using an object as the landmark.

steering angle, which uses the distance travelled on the path to the point S as a parameter, and to determine the position of S which satisfies the measurement results. The problem with this method is the error in predicting the position and attitude using the information from the steering angle.

(iii) To determine the position of S by providing the direction of the travel path at point S against the O-XY coordinate system, with combined use of a sensor, such as a gyrocompass, which can determine the direction. For travel over a relatively short distance, a rate gyro will detect the direction with reasonable accuracy. Therefore this method is considered to be practical.

As mentioned above, there are several methods of determining the current position of a moving body. These measurement errors from the specified point can be corrected by redesigning the route to the next destination.

6. CONCLUSIONS

A navigation method for mobile robots which uses discrete landmarks has been proposed and path navigation between two points, and a mark position measuring method using cylindrical poles and flat faces of buildings in the operation environment for landmarks have been discussed. A travelling error detection method that uses these landmarks has also been proposed. In this work, cylinders and flat surfaces were used for the objects of the sensor which are generally found in an operation environment and serve as satisfactorily efficient objects. Optical sensors, instead of ultrasonic sensors, also provide satisfactory sensing, and the principle of the navigation system is the same for either sensor. When cylinders are used as landmarks, the combined use of sensors, such as a gyrocompass, which determines the direction, is considered ideal. However, when landmarks such as walls, which enable detection of the direction of the robot, are used as landmarks, the use of ultrasonic sensors, in combination with the encoders used as simple interior sensors, will permit flexible travelling. Actually, successful navigation testing was accomplished over several tens of meters of loop passage, including curves using the actual passages in a building.

Acknowledgements

The authors would like to thank Mr Choichiro Soda, Director of Machinery Department, Mechanical Engineering Laboratory; Mr Minoru Abe, Director of Automobile Department; Mr Akio Fijikawa, Head of Mechanism Division; and the members of Mechanism Division. They are also grateful to Mr Masanori Hayashi, formerly of Daiho Ltd., who manufactured the experimental mobile robot for the experiments.

REFERENCES

1. Y. Oshima, E. Kikuchi, M. Kimura and S. Matsumoto, "Control system for automatic automobile driving," *Proc. IFAC*, pp. 347-357, 1965.
2. S. Yonekura, E. Maruyama, S. Ando and S. Kawano, "Development of optically guided robot vehicle, Hitachi Hoiverser," *The Hitachi Hyoron*, vol. 75, no. 10, pp. 23-28, 1975 (in Japanese).
3. G. E. Forsen, "Processing visual data with an automaton eye," *Pictorial Pattern Recognition*, pp. 471-502, 1968.
4. T. Nozaki, "Automatic driving of an automobile that has a function to recognize obstacles," *Trans. Soc. Instrum. Contr. Engineers*, vol. 13, no. 5, pp. 475-481, 1977 (in Japanese).

5. K. Kakegawa and Y. Kanayama, "Automatic construction of a map by autonomous mobile robot, 'YAMABICO 9,'" *Proc. 1st Conf. Robotics Soc. Jpn.*, pp. 199–202, 1983 (in Japanese).
6. K. Matsushima and M. Oda, "Route searching of unknown environment using tactile information," *Proc. Symp. Intelligent Mobile Robot*, pp. 65–70, 1982 (in Japanese).
7. S. Tachi, K. Komoriya, K. Tanie, T. Ohno and M. Abe, "Guide dog robot—feasibility experiments with MELDOG MARK III," *Proc. 11th ISIR*, pp. 95–102, 1981.

ABOUT THE AUTHORS



Kiyoshi Komoriya was born in Tokyo, Japan, on 7 July 1951. He received B.S. and M.S. degrees in mechanical engineering from the University of Tokyo in 1974 and 1976, respectively. In 1976 he joined the Mechanical Engineering Laboratory, Ministry of International Trade and Industry, Tsukuba Science City, Japan, and is currently a Senior Research Scientist of the Cybernetic Division of the Robotics Department. He is a member of the Japan Society of Mechanical Engineers, the Society of Instrument and Control Engineers, and of the Society of Biomechanisms. His research interests include man-machine systems and robotics, especially motion control of mechanisms and the intelligence of a mobile robot.



Susumu Tachi was born in Tokyo, Japan, on 1 January 1946. He received B.E., M.S. and Ph.D. degrees in mathematical engineering and instrumentation physics from the University of Tokyo in 1968, 1970 and 1973, respectively. He joined the Faculty of Engineering, University of Tokyo, in 1973. From 1973 to 1976 he held a Sakkokai Foundation Fellowship. In 1975 he joined the Mechanical Engineering Laboratory, Ministry of International Trade and Industry, Tsukuba Science City, Japan, and is currently Director of the Man-machine Systems Division of the Robotics Department. From 1979 to 1980 he was a Japanese Government Award Senior Visiting Fellow at the Massachusetts Institute of Technology, Cambridge, U.S.A. His present interests include human rehabilitation engineering, statistical signal analysis and robotics, especially sensory control of robots, rehabilitative robotics and the human robot system. Dr Tachi is a member of IEEE, the Japan Society of Medical Electronics and Biomedical Engineering, the Society of Instrument and Control Engineers, the Japan Society of Mechanical Engineers, and of the Society of Biomechanisms.



Kazuo Tanie was born in Yokohama, Japan, on 6 November 1946. He received B.Sc., M.Sc. and Dr. Eng. degrees in mechanical engineering from Waseda University, Tokyo, in 1966, 1971 and 1980, respectively. He joined the Mechanical Engineering Laboratory, Ministry of International Trade and Industry, Tsukuba Science City, Japan, in 1971 and is currently Director of the Cybernetics Division of the Robotics Department. He is also a Visiting Lecturer of Utsunomiya University. He was a Visiting Scholar of the Biotechnology Laboratory, University of California at Los Angeles from August 1981 to August 1982. His interests currently relate to sensor, mechanisms and control in robotics and rehabilitation engineering. Dr. Tanie is a member of the Japan Society of Medical Electronics and Biomedical Engineering, the Society of Instrument and Control Engineers, the Japan Society of Mechanical Engineers, and of the Society of Biomechanisms.